Available online at www.sciencedirect.com
SCIENCE DIRECT®

Journal of the European Ceramic Society 24 (2004) 393–397

www.elsevier.com/locate/jeurceramsoc

Microstructure after superplastic creep of alumina–zirconia composites prepared by powder alcoxide mixtures

J.M. Calderon-Moreno[a,*], M. Schehl[a,b]

[a]*INCAR (CSIC), La Corredoria, s/n Oviedo, Spain*
[b]*Institut für Verbundwerkstoffe GmbH, Erwin-Schrödinger-Strasse, 67663 Kaiserslautern, Germany*

Abstract

The microstructural evolution during superplastic creep of alumina–zirconia composites prepared from alumina powder–zirconium alcoxide mixtures was studied, in order to determine the changes in the grain size and shapes. Zirconia reinforced alumina composites with up to 20 wt.% ZrO_2 content were deformed in compression creep tests at constant load in air at 1350 °C. The microstructure was studied by means of SEM. The distribution of both phases, grain sizes and shapes were determined on sintered and tested materials. Grain size distributions are narrow, with typical zirconia particle sizes several times finer than alumina ones, resulting in intergranular small zirconia grains occupying most alumina triple points. Every composition was deformed in stationary creep to 100% true strain. Superplastic strains were achieved by the coupled dynamic movement of grains during grain boundary sliding and simultaneous accommodation at triple points by zirconia particles. The shape and size changes in alumina and zirconia grains revealed that transport of matter took place also by diffusion at the grain boundaries. Grain boundary diffusion at alumina–zirconia interphases resulted in significant grain shapes in the zirconia particles, with zirconia grains exhibiting protruding parts along the alumina grain boundaries aligned perpendicularly with the compression axis.

Keywords: Alkoxides; Al_2O_3–ZrO_2; Creep; superplasticity

1. Introduction

Superplasticity remains essentially a phenomenological topic. This is partly due to the fact that ductility is not an intrinsic property of the material but depends of the time observation scale. During superplastic deformation the strain rate and therefore the flow stress are controlled by the diffusivity in grain boundaries. Superplasticity in a fine grained Al_2O_3/20%ZrO_2 composite was first reported by Wakai et al.,[1,2] at 1500 °C. Their finding opened the search for higher ductility at lower temperatures and increased strain rates. However the effect of zirconia particles on ductility it is not yet well understood, i.e. there are discrepancies in the literature about the relative sliding mobilities of the different interfaces in the composites. Recent studies in composites with zirconia addition from 1000 ppm up to 20% have clarified the different role of zirconia as a dopant and in the form of zirconia particles dispersed in the composite.[3–13] It is now widely accepted that segregation of Zr^{4+} at grain boundaries takes place for very low contents and results in lower grain boundary diffusivity. Elevated ductility has been reported from different authors in two-phase composites, while other authors reported the inhibition of plastic deformation and the increase of flow stress.

Considerations solely based on flow stress are simplistic. Fine grain size is necessary to observe reduced flow stress at a given strain rate and temperature and therefore desirable to obtain high ductility at a a lower temperature. It is also well stablished that even 0.1% zirconia addition hinders the grain growth of alumina.[10] The critical factor to obtain superplastic composites is the microstructural homogeneity, namely both the spatial distribution of zirconia particles and the grain size distribution of both alumina and zirconia. It has then to be stressed the importance of the used processing route.

The effect on creep of the processing method comparing the behaviour of Al_2O_3/5.5v%ZrO_2 composites processed by powder mixing and sol-gel was previously studied.[14] An homogeneous distribution of fine zirconia particles and narrow grain size distributions resulted in the extention toward higher stresses of the stress range

* Corresponding author. Present address: Departamento de Ciencia de Materiales, ETSEIB, UPC, Avda Diagonal 647, Barcelona 08028, Spain.
E-mail address: jose.calderon@upc.es (J.M. CalderonMoreno).

0955-2219/03/$ - see front matter © 2003 Elsevier Ltd. All rights reserved.
doi:10.1016/S0955-2219(03)00216-4

at which stationary creep rates could be observed. The maximun strains achievable by stationary creep without creep damage also increased, without affecting significantly the creep rates at low stresses. A small addition of zirconia particles by colloidal methods also increased the ductility in alumina and silicon carbide whisker reinforced alumina composites.[15] In the present research alumina–zirconia composites were obtained by powder alcoxide mixtures. Alumina grain sizes were ~1 μm and zirconia grains around 0.2 μm were located at alumina triple points. The composites were deformed to 100% true strains at 1350 °C and the microstructures after creep were studied. The microstructural evolution of the binary composites during creep is presented.

2. Materials and experimental

The processing of polycrystalline alumina zirconia composites was carried out mixing high purity (99.995%) alumina powder and zirconium alcoxides.[16,17] Nearly fully dense samples were obtained. Densification took place by presureless sintering at 1600 °C. The composites were named after their zirconia content: AxZ, with 'x' being the wt.% of zirconia. Polished surfaces of as-received and deformed samples were observed by SEM. Some were thermally etched in air at 1400 °C for 1 h to reveal grain morphology. Key microstructural features, zirconia distribution, grain size distribution of zirconia and alumina and shape of grains, were studied by means of an image analyzer, using between 200 and 600 grains for each measurement.

Mechanical tests were carried out on 2×2×4 mm^3 samples under compression using a Instron commercial apparatus. To avoid friction with the alumina pushing rods, the samples were sandwiched between well aligned and flat sapphire single crystals. All tests were performed at 1350 °C in air at a constant load of 50 MPa (initial engineering stress), until 100% strain and stopped when strain reached that level. Fracture occurred before 100% strain only in the monolithic alumina material.

3. Results

3.1. Microstructure of as-sintered samples

Fig. 1 shows a polished and etched surfaces of A20Z. Average alumina grain sizes ranged from 5.5 μm for A to 1.3 μm for A20Z and were fairly homogeneous thorough each composite. ZrO_2 grains are homogeneously distributed throughout the Al_2O_3 matrix with a typical particle size, $d_{average}$ [ZrO_2], from 200 nm in A5Z to more than 300 nm in A20Z, several times finer that the alumina grain size. They were located at alumina triple points. In the A5Z material more than one of every two triple points were occupied by zirconia particles, in the A10Z composite two of every three triple points were filled with zirconia particles and in A15Z and A20Z zirconia particles were present in nearly all triple points. The zirconia particle sizes were very homogeneous, with 90% of the particles between 0.5 $d_{average}$[ZrO_2] and 2 $d_{average}$[ZrO_2] in each composite. The alumina grain size distribution was also narrow, the maximum grain sizes observed were less than two and about two times the average grain size for zirconia and alumina, respectively.

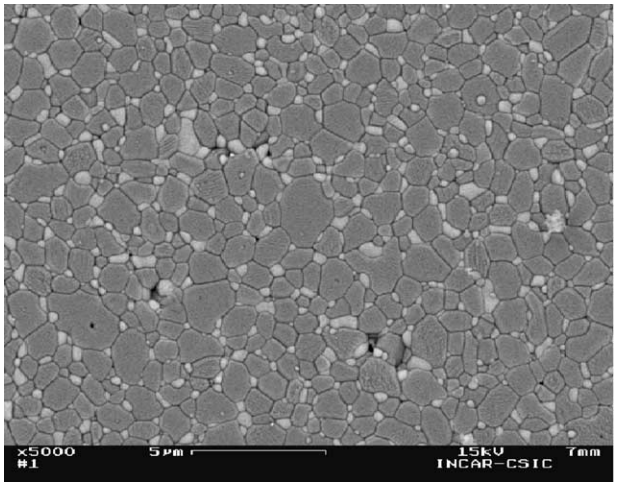

Fig. 1. SEM micrograph showing the polished cross-section of the A20Z composite prepared from powder alcoxides mixtures. The alumina grains (darker phase) have a grain size several times higher than the zirconia grains (brighter phase). Zirconia grains are placed mainly in the grain boundaries, although some intragranular zirconia can also be observed.

The addition of zirconia is very effective in hindering the grain growth of alumina during sintering, even for the lowest zirconia content. The addition of up to 20 wt.% ZrO_2 prevents grain growth without allowing the formation of zirconia agglomerates, which are very deletereous for the mechanical stability of the composite. The grain size distribution in the composites is illustrated in Fig. 2, while the evolution of particle size with zirconia content is shown in Fig. 3. A higher zirconia content is associated with the increase of zirconia grain sizes and the decrease in alumina grain sizes.

3.2. Microstructure of samples deformed to $\epsilon = 100\%$

After 100% strain all samples appeared neat and homogeneously deformed: all the faces remained parallel to their initial orientations and no rounded edges, no barrelling occurred. Small pores at triple points appear in the same proportion than in as-sintered samples. Fig. 4 shows a SEM micrograph after 100% strain. The

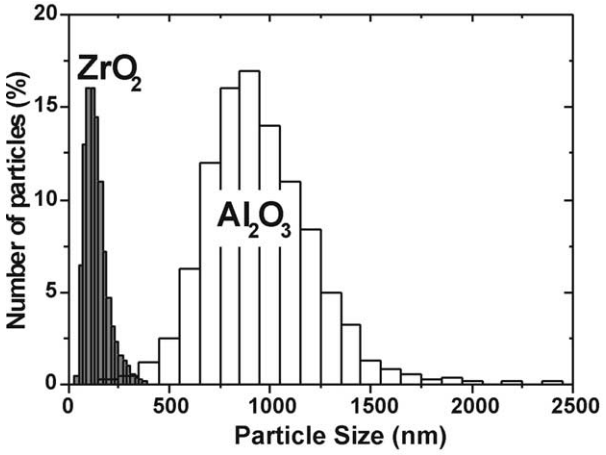

Fig. 2. Illustration of the relative particle size distribution of alumina and zirconia in the composites. The smaller alumina grains have similar size than the bigger zirconia grains.

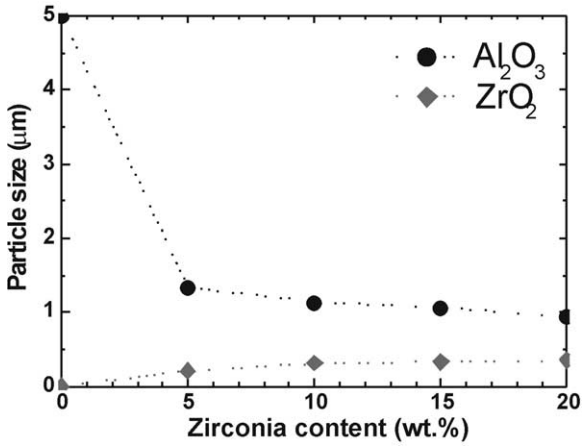

Fig. 3. Evolution of the average grain size of alumina and zirconia in the composites with increasing zirconia content (wt.%).

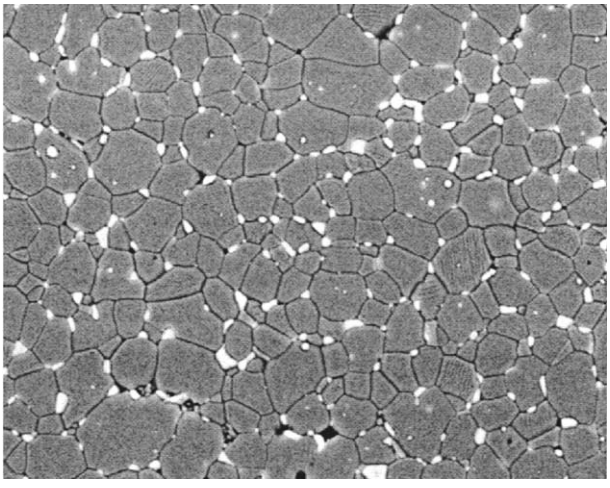

Fig. 4. SEM micrograph showing the polished cross-section of a composite deformed a strain $\epsilon = 100\%$.

apparent changes in the preliminary SEM observations of deformed samples were:

- A small change in grain size and a more rounded shape of alumina grains.
- Zirconia grains in the triple points between rounded alumina grains appeared squeezed.

Grain sizes and shapes in deformed samples were subsequently studied by SEM and measured by means of an image analyzer, in polished and etched cross-sections perpendicular and parallel to the compression axis, in order to determine any anisotropy in the grain size deformation, due to the uniaxial compressive stress. Fig. 5 shows SEM micrographs of the polished cross-section in both planes, relative to the compressive axis. Fig. 5A shows the same features than the preliminary observations, done only in the plane perpendicular to

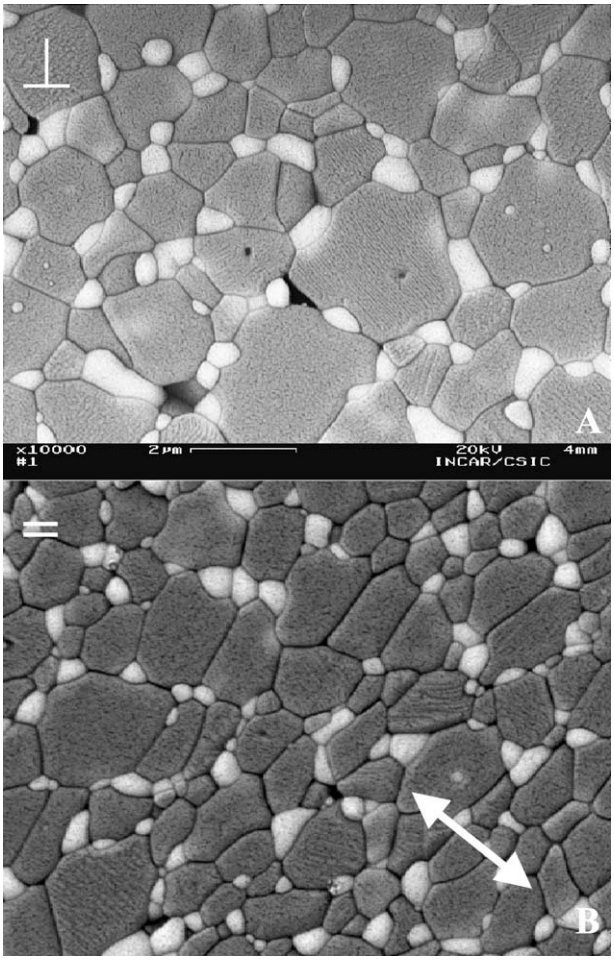

Fig. 5. SEM micrograph of deformed samples. (A) Cross-section in the plane perpendicular to the compression axis (called $\perp$). (B) Cross-section in the plane parallel to the compression axis (called $=$), showing the alignment of the grains along the axis perpendicular to the compression axis, indicated by an arrow in the figure.

the compression axis. Fig. 5B, in the plane parallel to the compression axis, shows the alignment of the grains along the axis perpendicular to the compression axis.

The evolution of the deformed grains reveals a change from equiaxed to a more lenticular shape. Fig. 6 illustrates the effect. The biggest and circular circular cross-section of the grains tend to lie in the plane perpendicular to the compression axis. The shape change, however, does not necessarily implies an associated change in the volume of the grains. The grain size evolution was investigated from the grain size distribution obtained in cross-sections perpendicullar and parallel to the compression axis in the deformed composites. Fig. 7 shows the evolution of alumina grain size in both cross-sections, compared to the intial grain size.

The particle size distributions of alumina and zirconia for the as-sintered A20Z and cross sections perpendicular and parallel to the compression axis in deformed samples composite are shown in Fig. 7. The differences in the apparent grain size in the different cross-sections were clear before and after testing. The particle size distributions indicate that the grain sizes become smaller in the = plane and bigger in the bottom plane. The average grain size after testing was defined as $d_{def} = (d_{=} d_{\perp}^{2})^{1/3}$, where $d_{=}$ and $d_{\perp}$ represent the average grain sizes measured in the parallel and perpendicular cross sections. When compared with the as-sintered value, $d_{def} = d_{as\text{-}received}$. We can conclude from the microstructure study that no change in grain size occurs. The apparent grain growth observed in the plane perpendicular to the compression axis corresponds to the change

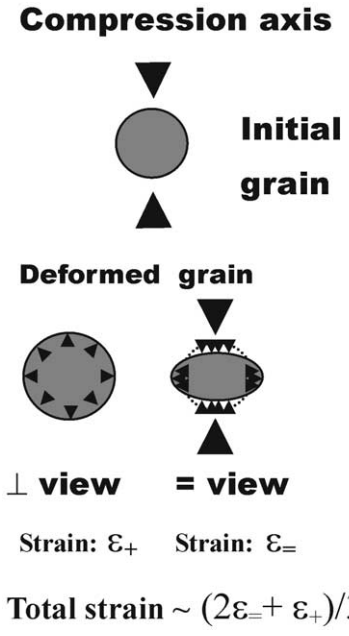

Fig. 6. Illustration of the change in grain shape from equiaxed to lenticular in the deformed samples. The shape change indicates the activity of diffusional.

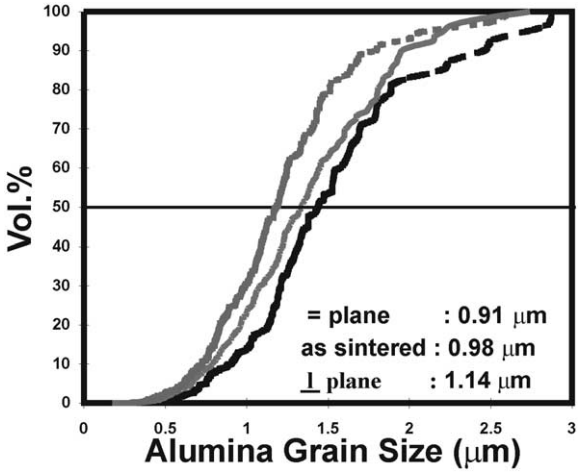

Fig. 7. Alumina grain size distribution in as-sintered and in deformed samples (in the = plane and in the ⊥ plane) showing the changes in grain shape in deformed samples, dcue to difffusional creep in uniaxial compression (Figs. 5 and 6).

of the shape of alumina equiaxed grains submitted to uniaxial stress, as shown in Fig. 6 and not to grain growth. The grains acquire a non equiaxed lenticular shape.

The changes in grain shape indicate that diffusional processes are active during creep. Diffusional transport of matter couples with grain boundary sliding to account for the total strain during creep. The contribution to the total strain due to diffusion within the grain can be approximately determined from the observed change in grain shapes after testing. A simple calculation reveals that the observed variation in average grain shape affects around 15% of the volume of the grain.

Many zirconia grains appeared significantly deformed after deformation (i.e. zirconia grains with protrudring fingers elongating along alumina grain boundaries were observed). This significantly higher grain shapes than in alumina grains can be attributed to a significanly higher diffusional activity accommodating grain boundary sliding taking place in the zirconia grains, relative to alumina grains. The internal features of alumina grains also indicated that diffusional transport of matter took place mainly at the grain boundaries, because the intragranular zirconia grains always appeared rounded and completely undeformed, in contrast with the intergranular zirconia at alumina grain boundaries.

4. Conclusions

Alumina/zirconia composites with a narrow distribution of alumina and zirconia grain sizes and an homogeneous microstructure of fine zirconia particles filling

almost all alumina triple junctions, due to the suitable zirconia/alumina grain size ratio, were obtained by powder alcoxide mixtures. The described intergranular zirconia microstructure is advantageous for achieving superplastic deformation without significant creep damage. The structural evolution after superplastic creep was presented.

The microstructural evolution of the studied composites during superplastic creep indicates a grain-boundary diffusion controlled deformation mechanism, coupled with grain boundary sliding. The results indicate that zirconia addition using advanced processing can significantly increase the ductility of alumina-based composites by controlling the relative grain size and distribution of both phases.

Acknowledgements

The authors would like to thank Dr. R. Torrecillas for helpful discussions. Financial support by the Spanish Ministry of Science and Technology is gratefully acknowledged.

References

1. Wakai, F., Sakaguchi, S. and Matsuno, Y., Superplasticity of yttria-stabilized tetragonal ZrO_2 polycrystals. *Adv. Ceram. Mat.*, 1986, **1**, 259–263.
2. Wakai, F., Superplasticity of Al_2O_3–ZrO_2 duplex composites. *J. Jpn Soc. Powder & Powder Met.*, 1991, **38**, 643.
3. Chen, I. W. and Xue, L. A., Superplastic alumina ceramics with grain growth inhibitors. *J. Am. Ceram. Soc.*, 1990, **73**, 2585–2609.
4. Kim, B. N., Hiraga, K., Morita, K. and Sakka, Y., Superplasticity in alumina enhanced by co-dispersion of 10% zirconia and 10% spinel particles. *Acta Mat.*, 2001, **49**, 887–895.
5. Xue, L. A. and Chen, I. W., Superplastic alumina at temperatures below 1300 °C using charge-compensating dopants. *J. Am. Ceram. Soc.*, 1996, **79**, 233–238.
6. Wakai, F., Nagano, T. and Iga, T., Hardening in creep of alumina by zirconium segregation at the grain boundary. *J. Am. Ceram. Soc.*, 1988, **90**, 2361–2366.
7. Okada, K. and Sakuma, T., Tensile ductility in zirconia-dispersed alumina at high temperatures. *J. Am. Ceram. Soc.*, 1996, **79**, 499–502.
8. Nakano, K., Suzuki, T. S., Hiraga, K. and Sakka, Y., Superplastic tensile ductility enhanced by grain size refinement in a zirconia-dispersed alumina. *Scripta Mater.*, 1997, **38**, 33.
9. Baddi, R., Clarisse, L., Duclos, R. and Crampon, J., Superplastic deformation during creep of alumin–zirconia composites. In *Third Euroceramics, Vol. 3*, ed. P. Duran and J. F. Fernandez. Faenza Editorial, Spain, 1993, pp. 641–646.
10. Flacher, O., Blandin, J. J. and Plucknett, K. P., Effects of zirconia additions on the superplasticity of alumina–zirconia composites. *Mat. Sci. Eng. A*, 1996, **221**, 102–112.
11. Chevalier, J., Olagnon, C., Fantozzi, G. and Cross, H., Creep behaviour of alumina, zirconia and zirconia-toughened alumina. *J. Eur. Ceram. Soc.*, 1997, **17**, 859–864.
12. Sakka, Y., Suzuki, T. S., Morita, K., Nakano, K. and Hiraga, K., Colloidal processing and superplastic properties of zirconia- and alumina-based nanocomposites. *Scripta Mat*, 2001, **44**, 2075–2078.
13. Tai, Q. and Mocellin, A., Review: high temperature deformation of Al_2O_3-based ceramic particle or whisker composites. *Ceram. Int.*, 1999, **25**, 395–408.
14. Calderón Moreno, J. M., DeArellano-López, A. R., Domínguez-Rodríguez, A. and Routbort, J. L., Microstructure and creep properties of alumina/zirconia ceramics. *J. Eur. Ceram. Soc.*, 1995, **15**, 983–988.
15. Calderón Moreno, J. M., DeArellano-López, A. R., Domínguez-Rodríguez, A. and Routbort, J. L., High temperature deformation of silicon carbide whisker composites fabricated by two different techniques. *Mat. Sci. Eng. A*, 1996, **209**, 111–115.
16. Schehl, M., Diaz, L. A. and Torrecillas, R., Alumina nanocomposites from powder-alkoxide mixtures. *Acta Mat.*, 2002, **50**, 1125–1139.
17. Calderon-Moreno, J. M., Schehl, M. and Popa, M., Microstructure and superplastic stationary creep at 1350°C of alumina-zirconia composites prepared by powder alcoxide mixtures. *Acta Mat.*, 2002, **50**, 3973–3983.